Textures and Microstructures, 1993, Vol. 20, pp. 155–163
Reprints available directly from the publisher.
Photocopying permitted by license only

SPATIALLY RESOLVED TEXTURE ANALYSIS OF ALUMINUM–LITHIUM SHEET

S. M. MIYASATO, J. LIU and F. BARLAT

Aluminum Company of America, Alcoa Technical Center, Alcoa Center PA 15069

The yield strength anisotropy of aluminum–lithium sheet is known to be strongly dependent on crystallographic texture and grain morphology. In this study, the microstructure and texture of unrecrystallized and recrystallized variants of 2090 were examined in an SEM, using a combination of backscattered electron imaging and Kikuchi patterns. Local orientation measurements both through the sheet thickness and parallel to the rolling direction were used to determine the degree of misorientation between nearest-neighbor grains. Yield strength predictions based on the spatially resolved texture measurements show that the course, recrystallized grains have reduced in-plane and through-thickness anisotropy compared to the unrecrystallized structure.

KEY WORDS Aluminum–lithium, anisotropy, recrystallization, EBSP

1. INTRODUCTION

The aluminum–lithium system has three major advantages: low density, high stiffness, and relatively high strength. For these reasons, aircraft and aerospace industries have been investigating the potential use of aluminum–lithium for the past decade. However, there are several drawbacks to aluminum–lithium alloys, including poor ductility and low fracture toughness (Sanders and Starke, 1989). A disadvantage which is receiving increasing attention is the anisotropy in mechanical properties, which is severe in aluminum–lithium alloys (Peel *et al.*, 1983; Palmer *et al.*, 1980). Usually, airframers want the properties to be similar in all test directions. In aluminum–lithium, however, the difference between YS at 55° to RD can be as much as 15% below that in the 0° test orientation (Peel *et al.*, 1983). The strong effect of crystallographic texture on mechanical properties of Li-containing aluminum alloys has often been cited (Palmer *et al.*, 1980; Fox *et al.*, 1986; Peters *et al.*, 1986).

In addition to the in-plane anisotropy, aluminum–lithium product often display a through thickness anisotropy as well (Vasudevan *et al.* 1988). The center of a 13 mm thick plate of 2090 was observed to have a higher yield stress at mid-thickness than at the plate surfaces, which paralleled the intensity of the brass component. It was also suggested that the distribution of T_1 (Al_2CuLi) strengthening precipitates influences the degree of through-thickness anisotropy (Vasudevan *et al.* 1988). A gradient in texture has also been observed through the thickness of 2.15 mm 2090 sheet (Bowen 1990).

The pronounced crystallographic texture and high degree of mechanical fibering in thin 2090 product affect the yield strength (Fox *et al.*, 1986; Robertson, 1991). One way to change both the grain structure and the texture of the material

is to recrystallize the material. Recrystallization will probably lead to a more equiaxed grain structure, and a weaker crystallographic texture, both of which should reduce the anisotropy in the material. Thus, this study compares the grain structure and crystallographic texture of unrecrystallized and recrystallized variants of an aluminum–lithium based material, then predicts the yield strength at various directions to evaluate the mechanical anisotropy.

To characterize the difference in crystallographic texture between these two materials (unrecrystallized and recrystallized), the local orientation technique involving Electron Backscattered Patterns, or EBSP (Dingley, 1984) was used. This facility has already been described in the literature (Hjelen, 1990). The major advantage of this system is the ability to simultaneously image the grain structure of the specimen and display the Kikuchi band patterns so that a one-to-one correlation can be made between the imaged grain and the crystallographic orientation.

2. EXPERIMENTAL PROCEDURE

Specimens were mounted with the plane normal to the long transverse direction exposed for analysis. Specimens were ground to 0.1 μm, then electropolished in 25% nital at -20°C for 30 seconds with an applied potential of 10 V.

Analysis was performed in a JSM 840A, which was operated at 20 kV, equipped with an additional BSE detector and phosphor screen. For through-thickness analysis, at least 120 contiguous grains were analyzed. To characterize specific locations (i.e. surface and center), 160 randomly selected grains were analyzed for each location.

3. RESULTS

The structure of the unrecrystallized, commercial 2090 sheet is shown in Figure 1. The microstructure consists of high-aspect ratio grains elongated in the rolling direction. The backscattered SEM images also reveal a great deal of substructure. A comparison of the grain morphology near the surface of the sheet (Figure 1a) and the midthickness (Figure 1b) shows that there is a gradient in morphology: the grains at midthickness have a finer substructure with smaller aspect ratio than near-surface grains.

The recrystallized microstructure is shown in Figure 2. In comparison with the fully unrecrystallized microstructure, the grains are larger, considerably more equiaxed and show no substructure. The recrystallized grains still possess a tendency for elongation in the rolling direction, however. The recrystallization process also reduced the through-thickness gradient in grain morphology (compare Figures 2a and b); there are no distinguishing characteristics between the surface and midthickness microstructures.

The individual orientations measured at the surface and midthickness of the unrecrystallized sheet are contained in Figure 3. The $\langle 111 \rangle$ pole figure for the surface location appears asymmetric, with a strong Cu-type texture. The brass components, in comparison, are relatively weak. Also, the cube and goss

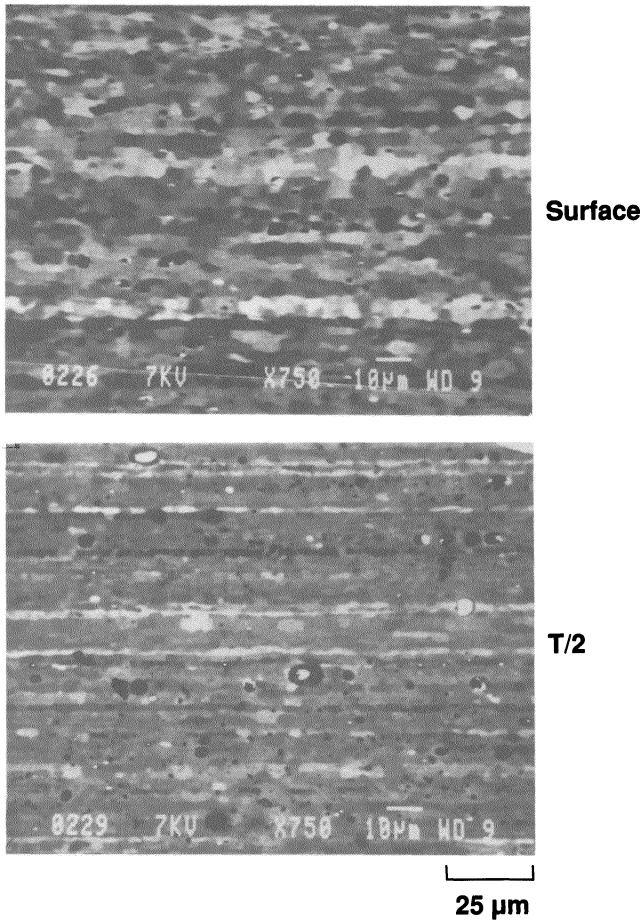

Figure 1 Optical micrographs of the unrecrystallized variant of 2090, at both the surface and center locations of the sheet, taken on the plane normal to the transverse direction.

recrystallization textures are not present; this is consistent with the results of Bowen (1990), who also observed no evidence of recrystallization (strong cube or goss textures) in 2.15 mm 2090 sheet. The pole figure from the center of the sheet is symmetric with strong brass components, which agrees with X-ray diffraction results for 2090.

The pole figures from the recrystallized material in Figure 4 are strikingly different from those in Figure 3. Instead of strong clusters of orientations, the orientations appear more randomly arranged at both surface and midthickness locations.

The orientation measurements of individual grains can be used to calculate the relative misorientation angle between grains in rows (parallel to the rolling direction) and in columns (parallel to the normal direction). Figure 5 shows a histogram of the misorientation angles measured in a column of 160 grains, from the surface to the T/4 location, in the unrecrystallized sheet. A substantial

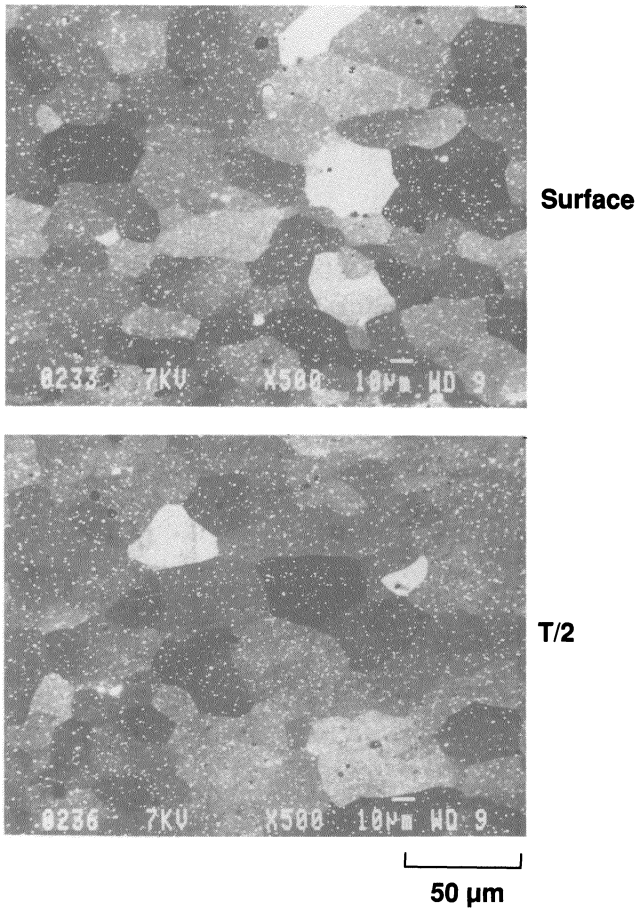

Figure 2 Optical micrographs of the recrystallized variant of 2090, at both the surface and center locations of the sheet, taken on the plane normal to the transverse direction.

number of grain boundaries are of low misorientation, e.g. ~25% of the boundaries have misorientation angles below 10°. One possible explanation is that recovery occurred during the thermomechanical processing of the sheet, and that subgrains are present in the structure. An alternate explanation is that the large strain deformation processes used to produce sheet caused grain rotation; thus, there would be a strong probability that neighboring grains would approach the same orientation.

In contrast to the large percentage of low angle boundaries observed in the unrecrystallized material, the majority of the boundaries in the recrystallized material are high angle. A histogram of the misorientation angles measured through the thickness of the sheet (surface to surface) is shown in Figure 6. The shape of the histogram resembles that of a randomly textured structure. The large misorientation angles verify that the microstructure is recrystallized.

Relative misorientation angles were also calculated between grains in rows.

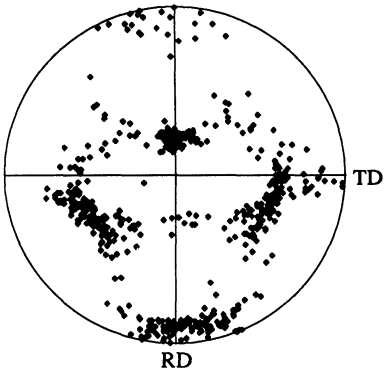

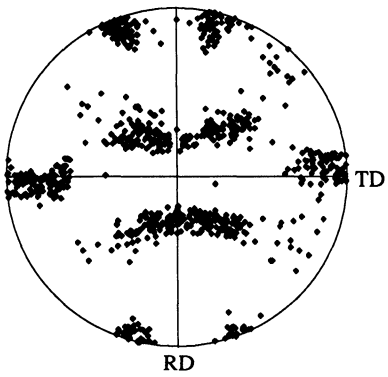

Figure 3 ⟨111⟩ pole figures from the surface (upper) and center (lower) planes of the unrecrystallized material.

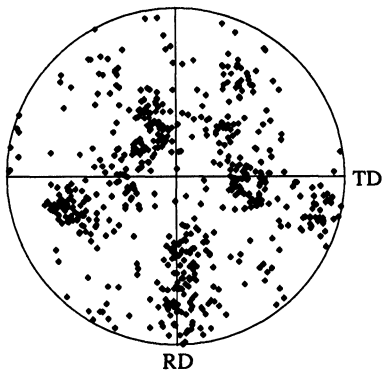

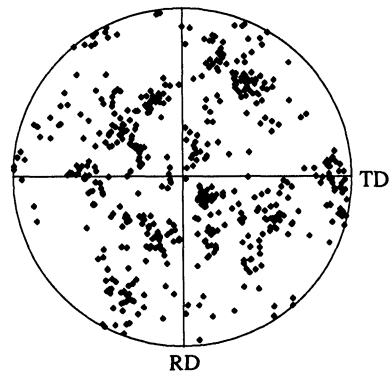

Figure 4 ⟨111⟩ pole figures from the surface (upper) and center (lower) planes of the recrystallized material.

Measurements were not made absolutely parallel to the rolling direction, but rather, followed "physically meaningful" rows. Thus, these results may be different from results obtained from completely automated measurements, which do not follow the rows of grains. Figure 7 shows histograms of misorientation angles between grains in the same row for the unrecrystallized material at both the surface and midthickness locations. Nearly all the boundaries analyzed were of low angle at both positions in the sheet. There seem to be more boundaries with less than 10° misorientation at the T/2 position (97%) than at the surface (67%) of the sheet.

Misorientation angles along rows of grains in the recrystallized material are seen in Figure 8. The coarse, recrystallized grains in this material did not lie in clearly defined rows. There were still a large number of boundaries of low angle in the rolling direction: 18% of grains at the surface and 37% at midthickness were of less than 10°. These values are larger than that expected in a completely random texture.

With the measured crystallographic texture, the yield strengths in different loading directions can be predicted using the Taylor, Bishop and Hill model. Figure 9 displays the predicted in-plane yield strength anisotropy for the

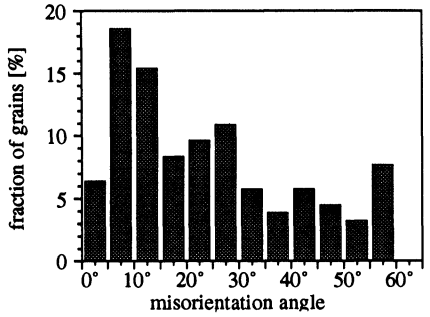

Figure 5 Grain-to-grain misorientation angle measured through the thickness of the unrecrystallized material.

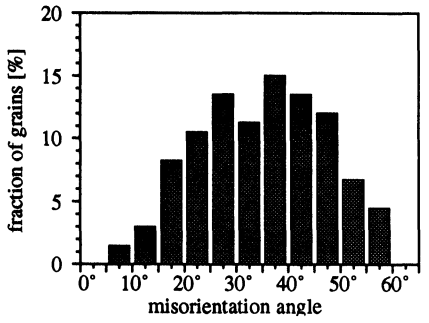

Figure 6 Grain-to-grain misorientation angle measured through the thickness of the unrecrystallized material.

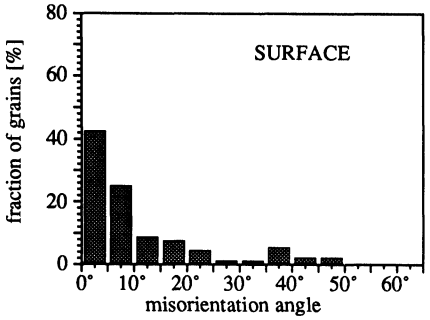

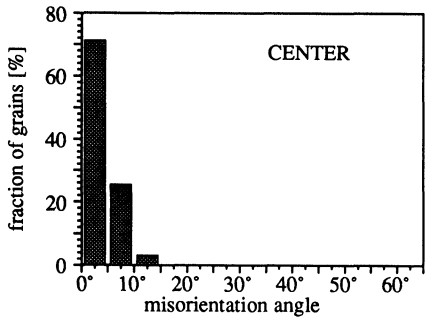

Figure 7 Grain-to-grain misorientation angle measured parallel to the rolling direction in the unrecrystallized material.

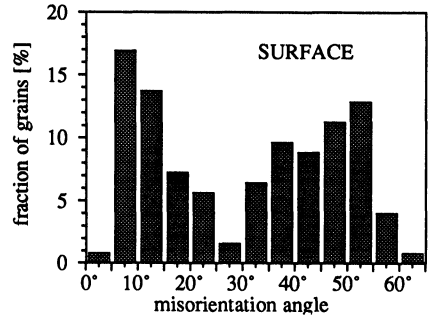

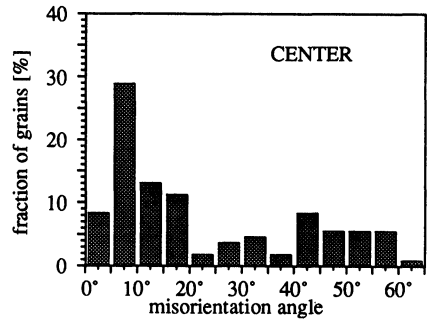

Figure 8 Grain-to-grain misorientation angle measured parallel to the rolling direction in recrystallized material.

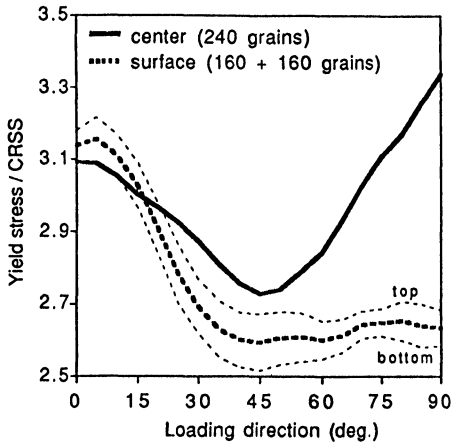

Figure 9 Predicted yield strength anisotropy of the unrecrystallized microstructure, as the loading axis varies from the rolling direction to the transverse direction.

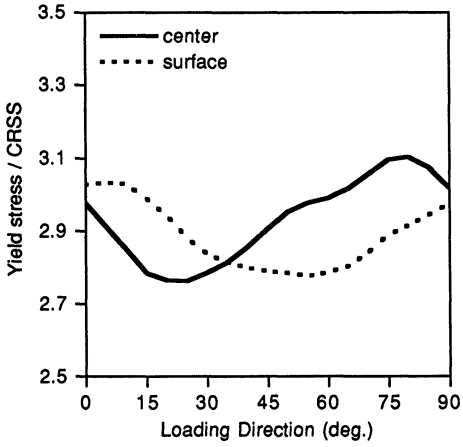

Figure 10 Predicted yield strength anisotropy of the recrystallized microstructure, as the loading axis varies from the rolling direction to the transverse direction.

unrecrystallized material at the surface and midthickness positions. The two curves display different behaviors, reflecting the differences in crystallographic texture between sheet surface and center. The (normalized) yield strength at the surface possesses maxima for stress directions 0° and 90° to the rolling direction, with a minimum at 45°. The yield strength of the center section of the sheet is also predicted to decrease from 0° to 45°, but does not recover strength with increasing angle from the rolling direction.

Figure 10 shows that the recrystallized material is predicted to have less anisotropic yield behavior than the unrecrystallized material. The difference between maximum and minimum points on the curve has been decreased by the recrystallization process. The recrystallized material still possesses both in-plane anisotropy and through-thickness anisotropy, since the curves in Figure 10 are not superposed.

4. DISCUSSION

The strong development of texture in aluminum–lithium alloys has been recognized for some time. However, it is only recently that the tools to characterize the microstructure and local texture have become available for studying commercially viable alloys.

The unrecrystallized material had several characteristics. Backscattered electron imaging revealed elongated grains with significant substructure development, and the grains were thinner and more elongated near the surface of the sheet than at the center. Grain morphology is often cited in the literature as a factor in determining whether the structure is unrecrystallized or recrystallized. However, grain shape is only an indicator of the recrystallized nature. The combination of local texture information and grain morphology gives more

information about the nature of the grain structure. The unrecrystallized microstructure exhibited a strong crystallographic texture, as displayed by the pole figures. The nearest neighbor misorientations, however, give the strongest evidence that the structure did not recrystallize. Thus, low angle boundaries are encountered in the rolling direction with high frequency, and in the normal direction with lower frequency.

Similarly, the combination of grain imaging and local orientation determination led to an improved understanding of the recrystallized structure. The recrystallized microstructure exhibited a weak, nearly random texture, as displayed by the pole figures. The nearest neighbor misorientations were mostly high angle in both the rolling and normal directions, as would be developed by recrystallization processes.

Predictions of yield strength suggest that the recrystallized variant has a reduced anisotropy, both in-plane and through-thickness. Recrystallization was also found to reduce the in-plane mechanical property anisotropy in Al–2.5Li–1.8Cu–0.7Mg–XZr sheet (Palmer *et al.*, 1986). However, the degree of anisotropy in Mg-containing aluminum–lithium alloys is not as high as in Mg-free aluminum–lithium alloys (such as 2090). For example, even in the completely unrecrystallized condition, Palmer *et al.* obtained a maximum:minimum ratio in yield strength of only 1.18 (360 MPa:305 MPa).

The predicted yield strength anisotropy results presented in Figures 9 and 10 have not been verified by experimental results. The yield strength predictions are based solely upon the local orientation measurements, and several other contributions to yield strength have been ignored (e.g. precipitation, grain morphology, etc). The material condition that should be used to check the validity of the prediction is the as-solution heat treated condition, with no stretch or artificial aging. One final note: in this work, we have only been concerned with the reduction in yield strength anisotropy. Although the calculations suggest that the degree of anisotropy in yield strength may have been reduced by recrystallization, it has been shown that recrystallization results in a general decrease in yield strength as well (Lin *et al.*, 1982).

5. CONCLUSIONS

The microstructure and texture of unrecrystallized and recrystallized variants of 2090 were analyzed using both backscattered electron imaging and Kikuchi patterns. The following results were obtained.

Measured grain-to-grain misorientation angles verify the unrecrystallized and recrystallized nature of the materials examined.

Unrecrystallized material had a gradient in both grain morphology and texture through the thickness, which contributes to yield strength anisotropy. In comparison, the recrystallized material had no observable gradient in either grain morphology or texture, and consequently is predicted to have reduced anisotropy.

ACKNOWLEDGEMENTS

The invaluable assistance of R. A. Burns and T. C. Connor is gratefully acknowledged.

References

Bowen, A. W. (1990). "Annex: Texture Analysis of 2090-T8E41 Aluminium–Lithium Alloy Sheet", *Short-Crack Growth Behaviour in Various Aircraft Materials,* AGARD Report No. 767, P. R. Edwards and J. C. Newman, Jr., eds., August 1990.

Dingley, D. J. (1984). *Scanning Electron Microscopy,* **1984/II,** 569–575.

Fox, S., McDarmaid, D. S. and Flower, H. M. (1986). Proc. Aluminum Technology '86, Book 3, The Institute of Metals, London, p. 72.1.

Fox, S., Flower, H. M. and McDarmaid, D. S. (1986). Proc. of the International Conference on Aluminum Alloys—Their Physical and Mechanical Properties, Charlottesville, VA, 939–950.

Hjelen, J. (1990). "Teksturutviking i Aluminium Studert ved Elektronmikrodiffraksjon (EBSP) i Scanning Elektronmicroskop", Norwegian Institute of Technology, PhD Thesis.

Lin, F. S., Charkraborty, S. B. and Starke, E. A. (1982). "Microstructure-Property Relationships of Two Al-3Li-2Cu-XCd Alloys", *Metall. Trans.*, **13A,** 401–410.

Palmer, I. G., Lewis, R. E. and Crooks, D. D. (1980). Proc. of the First International Aluminum–Lithium Conference, Stone Mountain, GA, eds. T. H. Sanders, Jr. and E. A. Starke, Jr., May 19–21, TMS-AIME, 241–262.

Palmer, I. G., Miller, W. S., Lloyd, D. J. and Bull, M. J. (1986). Proc. of the Third International Aluminum–Lithium Conference, eds. Baker, C., Gregson, P. J., Harris, S. J. and Peel, C. J., The Institute of Metals, 565–575.

Peel, C. J., Evans, B., Baker, C. A., Bennett, D. A., Gregson, P. J. and Flower, H. M. (1983). Proc. of the Second International Aluminum–Lithium Conference, Monterey, CA, eds. Sanders, T. H., Jr. and Starke, E. A., Jr., Apr. 12–14, TMS-AIME, 363–392.

Robertson, I. M. (1991). *Materials Forum,* **15,** p. 102.

Sanders, T. H., Jr. and Starke, E. A., Jr. (1989). Proc. of the Fifth International Aluminum–Lithium Conference, Williamsburg, VA, eds. Sanders, T. H., Jr. and Starke, E. A., Jr., Mar. 27–31, MCE Publications, Ltd., pp. 1–37.

Vasudevan, A. K., Fricke, W. G., Jr., Malcolm, R. C., Bucci, R. J., Przystupa, M. A. and Barlat, F. (1988). *Metall. Trans. A,* **19A,** 731–734.